The Effects of Variations in the Number and Sequence of Targeting Signals on Nuclear Uptake

Steven I. Dworetzky, Robert E. Lanford,* and Carl M. Feldherr

Department of Anatomy and Cell Biology, University of Florida, College of Medicine, Gainesville, Florida 32610; and
*Department of Virology and Immunology, Southwest Foundation for Biomedical Research, San Antonio, Texas 78284

Abstract. To determine if the number of targeting signals affects the transport of proteins into the nucleus, *Xenopus* oocytes were injected with colloidal gold particles, ranging in diameter from 20 to 280 Å, that were coated with BSA cross-linked with synthetic peptides containing the SV-40 large T-antigen nuclear transport signal. Three BSA conjugate preparations were used; they had an average of 5, 8, and 11 signals per molecule of carrier protein. In addition, large T-antigen, which contains one signal per monomer, was used as a coating agent. The cells were fixed at various times after injection and subsequently analyzed by electron microscopy. Gold particles coated with proteins containing the SV-40 signal entered the nucleus through central channels located within the nuclear pores. Analysis of the intracellular distribution and size of the tracers that entered the nucleus indicated that the number of signals per molecule affect both the relative uptake of particles and the functional size of the channels available for translocation. In control experiments, gold particles coated with BSA or BSA conjugated with inactive peptides similar to the SV-40 transport signal were virtually excluded from the nucleus. Gold particles coated with nucleoplasmin, an endogenous karyophilic protein that contains five targeting signals per molecule, was transported through the nuclear pores more effectively than any of the BSA-peptide conjugates. Based on a correlation between the peri-envelope density of gold particles and their relative uptake, it is suggested that the differences in the activity of the two targeting signals is related to their binding affinity for envelope receptors.

It was also determined, by performing coinjection experiments, that individual pores are capable of recognizing and transporting proteins that contain different nuclear targeting signals.

THE nuclear pore complex has been identified as the major, if not the exclusive site for macromolecular diffusion and transport between the nucleus and cytoplasm of eukaryotic cells (6, 10, 27). Evidence for mediated protein transport was determined initially for RN1 (9) and nucleoplasmin (4), both of which are major karyophilic proteins found in amphibian oocytes. From electron microscopic analysis of the intracellular distribution of nucleoplasmin-coated gold particles, it was established that the transport channels, located in the centers of the pores, are at least 200 Å in diameter (10). In contrast, the channel has a functional diameter of ~90 Å with respect to diffusion (27).

Several laboratories have used recombinant DNA methodology and single amino acid substitutions to obtain probes useful for the localization and characterization of transport signals that target specific proteins to the nucleus. These approaches have been used to study nuclear uptake of the following proteins: nucleoplasmin (1, 3), SV-40 large T-antigen (14), the yeast regulatory proteins MATα2 (13) and GAL4 (33), yeast histones 2A and 2B (23), the yeast ribosomal protein L3 (24), polyoma large T-antigen (29), and the adenovirus Ela protein (20). Although there is no concensus signal, it appears that nuclear targeting is dependent on short, basic amino acid sequences.

Of the proteins listed above, SV-40 large T-antigen has been studied most extensively. Kalderon et al. (14) constructed hybrid proteins by linking various amino acid sequences found in SV-40 large T-antigen to the amino terminus of pyruvate kinase and found that the shortest sequence capable of targeting the enzyme to the nucleus was Pro-Lys-Lys^{128}-Lys-Arg-Lys-Val. Transport is especially sensitive to a point mutation at the Lys^{128} position (14, 16, 18). Amino acid mutations in the vicinity of the Lys^{128} position reduces, but does not necessarily abolish, transport of SV-40 large T-antigen into the nucleus. Roberts et al. (30) have shown that multiple copies of a partially defective signal can cooperate to enhance nuclear localization.

Lanford et al. (17) synthesized peptides that contained the SV-40 large T-transport signal and cross-linked them to several carrier proteins (ovalbumin, BSA, IgG, sIgA, ferritin, and IgM). When the conjugates were injected into the cytoplasm of cultured cells, all but IgM (970 kD) entered the

Dr. Steven Dworetzky's current address is Department of Cell Biology, University of Massachusetts Medical Center, 55 Lake Avenue, North, Worcester, MA 01655.

Table I. Protein Preparations Used as Coating Agents

Coating agent	Average No. of signals	Sequence conjugated to BSA
BSA	0	
BSA-WT_5	5	Cys-Gly-Tyr-Gly-Pro-Lys-Lys-Lys-Arg-Lys-Val-Gly-Gly
BSA-WT_8	8	
BSA-WT_{11}	11	
BSA-cT_7	7	Cys-Gly-Tyr-Gly-Pro-Lys-Asn-Lys-Arg-Lys-Val-Gly-Gly
BSA-cT_{13}	13	
BSA-WT_8 + cT_7*	3	
Large T-antigen	1 per monomer	
Nucleoplasmin	1 per monomer	

The underlined sequence represents the active (WT preparations) and inactive (cT preparations) SV-40 large T nuclear transport signal.
* A 1:3 dilution of WT_8/CT_7 gave an average number of three active signals per BSA molecule.

nucleus. Qualitative evidence, using indirect immunofluorescence, suggested that the number of signals per carrier protein can affect the rate of uptake. Goldfarb et al. (12) found that BSA conjugated with SV-40 large T-antigen signals accumulates in the nuclei of *Xenopus* oocytes with saturable uptake kinetics, suggesting the involvement of a receptor-mediated process.

Nucleoplasmin, a 110-kD pentameric karyophilic protein, also has been used extensively to study nuclear transport in oocytes (4, 10) and cultured cells (31, 34). It has recently been determined that each monomeric subunit contains one targeting signal (Dingwall, C., personal communication). Furthermore, removal of one or more signal domains by proteolytic cleavage markedly reduces the rate of nuclear uptake (4). The region containing the signal has been sequenced and although it is similar to the SV-40 targeting signal, it is not identical (Dingwall, C., personal communication).

The data summarized above suggest that variations in the nuclear targeting signal could significantly influence nucleocytoplasmic exchange of proteins. To better understand the nature of these effects, experiments were performed to determine how macromolecules containing different signal sequences and different numbers of signals interact with and modulate the properties of the nuclear pores. Various sized colloidal gold particles were coated with (*a*) BSA conjugated with different numbers of synthetic peptides containing the SV-40 targeting signal, (*b*) BSA conjugated with inactive SV-40 signals, (*c*) large T-antigen, or (*d*) nucleoplasmin. These tracers were microinjected into oocytes and their distribution within the oocytes was later determined by electron microscopy.

The data indicate that as the number of signals per molecule increases, both the relative uptake of the tracer particles into the nucleus and the functional size of the transport channels increase. The SV-40 and nucleoplasmin targeting sequences varied in their ability to facilitate transport. This could be related to differences in their binding affinity for nuclear envelope (pore) receptors. Double labeling experiments demonstrated that different targeting signals can be recognized by and transported through the same pore. Control experiments ruled out the possibilities of nonspecific exchange processes.

Materials and Methods

Xenopus laevis were purchased from Xenopus I (Ann Arbor, Michigan) and maintained as reported previously (8).

Colloidal Gold Coating Agents

The synthesis of peptides containing the SV-40 large T-antigen targeting signals and their conjugation to BSA was described in detail by Lanford et al. (17, 18). In brief, the 13 amino acid sequence was synthesized on a glycyl-Merrifield resin (21) using an automated peptide synthesizer (model Sam Two; Biosearch, San Rafael, CA). The synthetic peptides were conjugated to BSA using the heterobifunctional cross-linking agent m-maleimido benzoyl-*N*-hydroxysuccimide ester (Pierce Chemical Co., Rockford, IL). Dialysis in PBS followed by repeated concentration and dilution of the conjugates separated the unconjugated peptides from the carrier proteins. By varying the molar ratios of the reactants, different protein–peptide coupling ratios were obtained. Amino acid analyses were performed with an analyzer (model 7300; Beckman Instruments Inc., Palo Alto, CA) to obtain a number-average ratio of signal peptides to carrier protein BSA. The peptide to carrier protein ratios obtained by SDS-PAGE were similar to those calculated by amino acid analysis.

Large T-antigen was expressed in insect cells using the baculovirus expression vector system (19) and was purified by immunoaffinity chromatography as described previously (32). Nucleoplasmin was isolated using an anti–nucleoplasmin IgG affinity column as described previously (6). BSA used in the control experiments was purchased from Sigma Chemical Co. (St. Louis, MO).

The BSA conjugates used as coating agents are listed in Table I. The table shows the synthetic 13 amino acid sequence conjugated to BSA and the average number of peptides per BSA molecule. The synthetic peptide contains the seven amino acid sequence required for nuclear localization of the SV-40 large-T antigen (17). The conjugates denoted BSA-WT represent preparations that contain active nuclear targeting signals. In the BSA-cT conjugates, neutral asparagine was substituted for the second lysine (equivalent to Lys^{128} in SV-40 large T-antigen) in the synthetic peptide (see Table I). The resulting signal is similar to the mutation present in the SV-40(cT)-3 mutant (16) and is defective in transport. To obtain a coating agent containing an average of three active signals per BSA molecule, the BSA-WT_8 conjugate was diluted threefold with the BSA-cT_7 preparation before stabilizing the gold particles. The use of BSA-cT_7 rather than BSA alone to dilute the active signal assured that the overall properties (size and charge) of the gold particles were consistent with those of other tracers used in this investigation. Purified SV-40 large T-antigen, which has one signal per monomer, and nucleoplasmin, which has a different signal sequence, also were used as coating agents. BSA alone was employed as an additional control.

Preparation and Stabilization of Colloidal Gold

The colloidal gold fractions that contained particles 20–50 and 20–160 Å in diameter were both prepared by reducing chloroauric acid with a solution

*Table II. Volumes of Coating Agent (μl) Required to Stabilize 1 ml of Gold Sol**

Coating agents (concentration)	Fraction size			
	20–50 Å	20–160 Å	50–280 Å	120–280 Å
BSA (1.0 mg/ml)	60	–	–	–
BSA-WT_5 (1.3 mg/ml)	10	60	40	–
BSA-WT_8 (0.6 mg/ml)	30	150	150	20
BSA-WT_{11} (0.5 mg/ml)	–	200	–	15
BSA-cT_7 (1.4 mg/ml)	20	80	–	–
BSA-cT_{13} (0.6 mg/ml)	–	–	140	–
Large T-Ag (0.4 mg/ml)	–	400	–	–
Nucleoplasmin (0.6 mg/ml)	–	40	150	25

* These are average values intended to serve as a guide. The exact amounts of coating agents required for stabilization should be determined for each individual gold preparation.

of white phosphorus in ether (7). 50–280-Å gold particles were obtained by adding 2.5 ml of 0.6% gold chloride to a freshly prepared 20–160-Å fraction, 1 ml of additional reducing agent was then added, and the preparation was boiled for 2–3 min. Fractions containing 120–280-Å particles were prepared by reducing chloroauric acid with trisodium citrate, as described previously (6, 11). The 50–280- and 120–280-Å gold sols, were brought to pH 7.0 with 0.72 N K_2CO_3.

Before stabilization, all of the coating agents were either dialyzed against, or dissolved in, a low ionic strength buffer (7.2 mM K_2HPO_4 and 4.8 mM KH_2PO_4, pH 7.0). The volumes of the different agents required to stabilize 1 ml of the gold sols are listed in Table II. The procedure used to determine these volumes is outlined in Feldherr et al. (10).

After stabilization, the 20–160- and 50–280-Å preparations were centrifuged at 2,000 *g* at 4°C for 10 min to remove any aggregates of gold. Centrifugation of the 20–50- and 120–280-Å fractions was not necessary. In each instance, 5–7 ml of stabilized colloid were concentrated to 70–100 μl in Minicon concentrators (Amicon Corp., Danvers, MA) and dialyzed against intracellular injection medium (102 mM KCl, 11.1 mM NaCl, 7.2 mM K_2HPO_4, and 4.8 mM KH_2PO_4, pH 7.0) at 4°C before injection.

By extrapolating from data published by De Roe et al. (2) and correcting for additional mass contributed by the conjugated peptides, estimates were made of the number of BSA-WT_8 molecules adsorbed onto the surfaces of different size gold particles. For example, particles with diameters of 35, 80, 140, and 180 Å (the mean size of the four different gold preparations injected) would have 2, 8, 24, and 39 molecules of BSA conjugates, respectively. Knowing the number of BSA molecules adsorbed and the synthetic peptide to carrier protein ratios, it was possible to estimate the total number of SV-40 large T-antigen targeting signals on the different size gold particles; however, the proportion of signal actually available for transport (i.e., exposed signals) is not known. Since adsorption of protein to the gold is a nonspecific process, it is assumed that the different conjugates would distribute similarly along the surface of the particles. This assumption is consistent with the data reported by De Roe et al. (2) for a variety of different stabilizing agents.

Injection

Late stage 5 and 6 oocytes (5) were manually defolliculated in amphibian Ringer's solution and centrifuged at ~650 *g* for 8–10 min (15). The cells were then microinjected with ~40 nl of gold sol at a site adjacent to the nucleus and fixed at intervals of 15 min, 1 h, 6 h or 20 h. The tip diameters of the micropipettes were 10–15 μm.

Electron Microscopy and Analysis

The cells were fixed for electron microscopy and prepared for sectioning as described previously (6). Relative nuclear uptake of gold particles stabilized with the different coating agents was determined by counting particles in equal and adjacent areas of the nucleus and cytoplasm close to the site of injection. Yolk granules and mitochondria were excluded from the analyses. The counts are reported as nuclear/cytoplasmic ratios (N/C)[1]. The size distributions of particles present within the nucleus and cytoplasm were determined by direct measurement from electron micrograph negatives. The envelope to cytoplasm ratios were obtained by comparing the number of particles associated with the cytoplasmic surface of the envelope (i.e., at or within 650 Å of the nuclear surface) to the number of particles in an equal, randomly selected area of cytoplasm.

Negative staining with 1% phosphotungstic acid was used to estimate the thickness of the adsorbed protein coats.

Results

Cytoplasmic Injections of the Tracer Particles

It was determined initially that microinjection of ~40 nl of stabilized gold adjacent to the nucleus delivered a sufficient number of particles for electron microscopic analysis. The protein content of the injectate ranged from 50 to 300 ng depending on the size of the gold fraction and the specific coating agent used.

All preparations containing functional transport signals (BSA-WT conjugates, large T-antigen, or nucleoplasmin) were translocated into the nucleus through central channels located within the nuclear pores. In the region of injection, the particles were uniformly distributed in the cytoplasm; however, at longer time intervals, 6 and 20 h, the BSA-WT conjugates occasionally formed aggregates. The reason for this is not known, but it appeared to be dependent on the presence of active signals since similar aggregates were not observed with BSA-cT conjugates. At all time intervals, particles containing functional transport signals were present both within the pores and the nucleoplasm. With increasing time there was a concomitant increase in the number of particles present in the nucleus (data not shown). Gold coated with the BSA-cT conjugates or BSA alone were essentially excluded from the pores and nucleoplasm. These general distributions are illustrated in Figs. 1 and 2, which show the results obtained 1 h after injecting particles coated with BSA-WT_{11} and BSA-cT_7, respectively.

Relative Uptake

Quantitative analysis of the nuclear uptake of particles stabilized with different coating agents was performed on oocytes fixed 1 h after injection. This relatively short time interval reduced possible loss or redistribution of soluble cell components caused by the injection procedures (22). The N/C ratios obtained at 1 h do not represent equilibrium values since nuclear uptake was observed to increase with time, but reflect relative uptake of the tracer particles. Due to the size

1. *Abbreviation used in this paper*: N/C, nuclear/cytoplasmic.

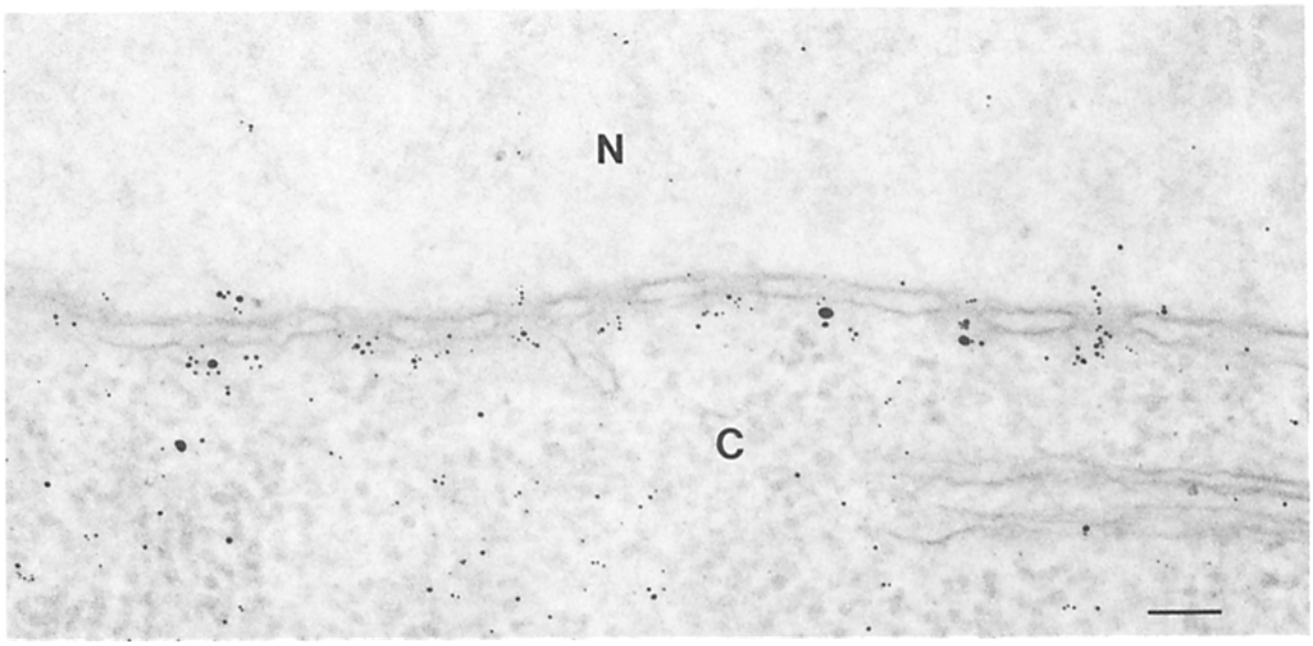

Figure 1. BSA-WT_{11}-gold (1-h experiment). Gold particles (20–160 Å) near the site of injection are observed to be evenly distributed throughout the cytoplasm (*C*). Particles are seen passing through the centers of the pores and also within the nucleus (*N*). Bar, 0.1 μm.

of the oocytes, the gold particles were not uniformly distributed throughout the entire cytoplasm within 1 h. To compensate for this factor, the nucleocytoplasmic regions selected for analysis were standardized and limited to areas within 250 μm of the injection site. Four to six cells were examined for each coating agent within each size fraction, and the experimental groups were compared statistically using the *t*-test.

The N/C ratios for different coating agents are given in Table III. After 1 h, N/C ratios obtained with the 20–50 Å fraction stabilized with BSA-WT_5 and BSA-WT_8 were 0.58 and 0.76, respectively, this difference is not statistically significant ($P > 0.25$). When the particle size was increased to 20–160 or 50–280 Å in diameter, the differences in N/C ratios between the BSA-WT_5 and BSA-WT_8 conjugates were highly significant ($P < 0.002$). In addition, BSA-WT_5 was more effective in facilitating transport than large T-antigen which contains one signal per monomer ($P < 0.002$). However, increasing the number of signals from 8 (BSA-WT_8) to 11 (BSA-WT_{11}) did not significantly increase the N/C ratio

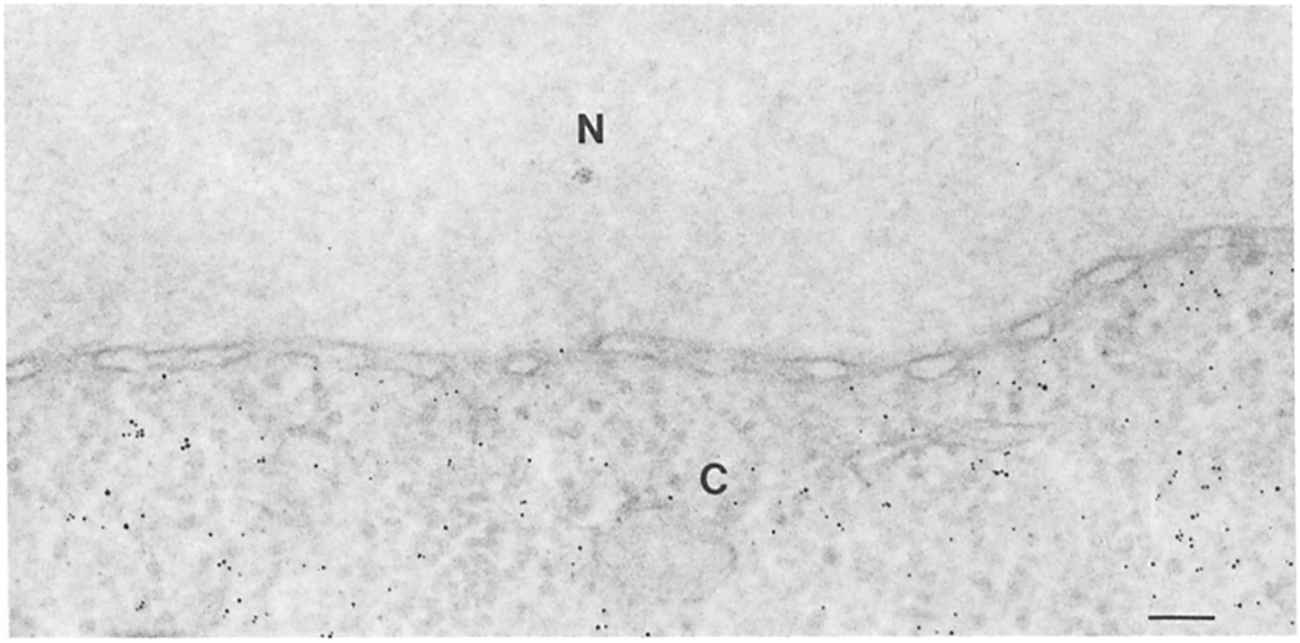

Figure 2. BSA-cT_7-gold (1-h experiment). Tracer particles (20–50 Å) near the site of injection are distributed evenly throughout the cytoplasm (*C*) but are rarely seen within the nucleus (*N*) or along the envelope. Bar, 0.1 μm.

Table III. N/C Ratios (1 h)*

Coating agents	Fraction size 20–50 Å	20–160 Å	50–280 Å	120–280 Å
BSA	0.009	–	–	–
BSA-cT_7	0.01	0.009	–	–
BSA-cT_{13}	–	–	0.006	–
BSA-WT_8 + BSA-cT_7 (1:3 dilution)	–	0.035	–	–
BSA-WT_5	0.58	0.18	0.06	–
BSA-WT_8	0.76	0.79	0.38	0.14
BSA-WT_{11}	–	0.80	–	0.24
Large T-antigen	–	0.077	–	–
Nucleoplasmin	–	2.43	0.71	0.51

* N/C ratios were calculated from 500 to 3,000 particle counts per data point.

(P values obtained for the 20–160 and 120–280 Å fractions were $P > 0.8$ and $0.1 > P > 0.05$, respectively). When comparing the results obtained with large T-antigen and the WT conjugates, it should be kept in mind that the availability of the targeting signals could be differentially affected as a consequence of adsorption to the surface of the gold.

The N/C ratio obtained for the BSA-WT_8-cT_7 dilution (an average of three signals per BSA molecule) was significantly lower than that obtained for the BSA-WT_5 conjugate ($P < 0.002$); however, it was also significantly lower than that observed for large T-antigen gold ($0.01 < P < 0.02$). The reason for the latter result is not known.

The N/C values for BSA-cT_7–, BSA-cT_{13}–, and BSA-coated gold were significantly lower than all gold preparations containing active nuclear targeting signals ($P < 0.002$).

Overall, it is concluded from these results that there is a direct correlation between the number of transport signals and the relative uptake of particles into the nucleus. Furthermore, the data suggest that as the size of the particles increases, more signals are required for their transport across the envelope.

To compare the effectiveness of a different targeting signal, parallel studies were performed with nucleoplasmin-gold. The relative uptake of different size nucleoplasmin-coated particles by the nucleus is shown in Table III. The N/C ratios determined for nucleoplasmin-coated particles were significantly greater than those obtained for BSA-WT_5–, BSA-WT_8–, or BSA-WT_{11}–coated gold. In all instances, the probability values were $P < 0.002$. Since there are only five targeting signals per nucleoplasmin molecule, these differences in uptake suggest that the nucleoplasmin transport signal is more effective than the SV-40 large T-antigen targeting sequence, at least in oocytes.

Size Distributions

In view of the above results, the size distributions of particles in different regions of the oocytes were analyzed in more detail. The nuclear and cytoplasmic size distributions determined for BSA-WT_5 and BSA-WT_8 1 h after injection are given in Table IV and Fig. 3. 17% of the BSA-WT_8–coated particles that entered the nucleus were >157 Å, compared to 5.6% for particles coated with BSA-WT_5. When particles >185 Å are compared, the difference in uptake is almost 10-fold. The difference in the size of the particles able to penetrate the pores is statistically significant as determined by Chi-square analysis.

When the number of signals per BSA molecule is increased beyond eight there is no further increase in functional pore size. This is indicated in Fig. 4, which compares the size distribution of BSA-WT_8–, BSA-WT_{11}–, and nucleoplasmin-coated particles within the nucleus 1 h after injecting a 120–280-Å gold fraction. The sizes of the particles able to pass through the pores did not vary significantly for the different coating agents. A comparison of the cytoplasmic distributions to the nuclear distributions, as shown in Table V, demonstrates that particles >230 Å (average of the size class), do not readily penetrate the pores, regardless of the coating agent. These results demonstrate that the maximum size particle able to enter the nucleus is ~260 Å in diameter. This value includes the thickness of the coat material, which adds ~30 Å to the overall particle diameter.

In contrast, the large T-antigen data given in Table VI indicate that particles >90 Å were not detected in the nucleus after 1 h. The size data obtained for the BSA-WT_8-cT_7 dilution experiment (Table VI) gave similar results, although a few particles >90 Å were present in the nucleus.

Overall, analysis of the size distributions of particles in the nucleus and cytoplasm indicate a direct relationship between the functional dimensions of nuclear pores and the number of active SV-40 large T targeting signals per BSA molecule.

Accumulation of Tracers Along the Nuclear Envelope

Although the nuclear size distributions were the same for particles coated with the BSA conjugates (WT_8 or WT_{11}) or nucleoplasmin, there was a significant difference in the relative uptake of the gold as a function of the coating agent, indi-

*Table IV. Size Distribution of BSA-WT_5– and BSA-WT_8–coated Particles in Injected Cells**

Experiment (1 h)	Total No. of particles measured	Percentage of particles in each size class‡ 45–73 Å	73–101 Å	101–129 Å	129–157 Å	157–185 Å	185–213 Å	213–241 Å	241–269 Å
BSA-WT_5									
Nucleus	406	31.5	19.7	24.6	18.5	4.9	0.7	–	–
Cytoplasm	533	3.2	11.1	24.2	29.8	14.8	9.0	3.8	1.1
BSA-WT_8									
Nucleus	1,018	14.3	20.3	24.6	23.8	10.1	4.8	1.7	0.4
Cytoplasm	808	5.2	13.1	25.0	28.2	14.7	7.4	3.6	1.7

* These experiments were performed with 50–280-Å gold particles; the mean size of the fraction was 140 Å.
‡ The size of the gold particles does not include the thickness of the coating agent.

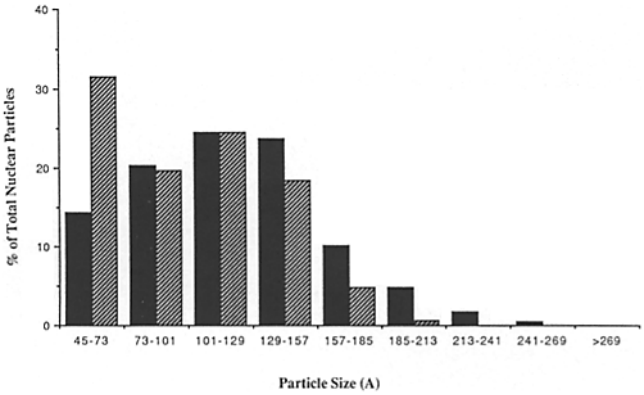

Figure 3. Nuclear particle size distribution: BSA-WT_8 (■) and BSA-WT_5 (▨).

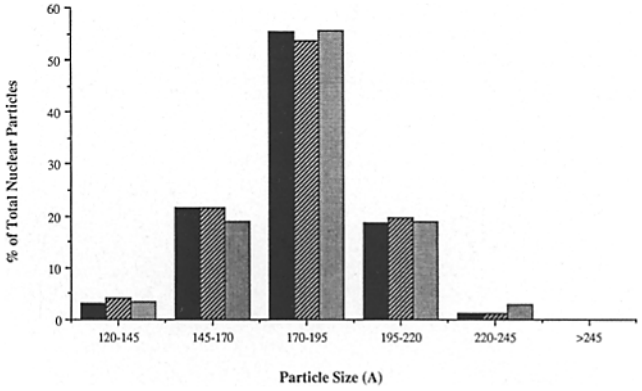

Figure 4. Nuclear particle size distribution: BSA-WT_8 (■), BSA-WT_{11} (▨), and nucleoplasmin (▩).

cating that not all transport signals are equally effective. The results shown in Fig. 5 and Table VII suggest that the effectiveness of specific signals could be related to their ability to bind to the nuclear envelope.

Fig. 5 illustrates the intracellular distributions of 50–280-Å gold particles coated with BSA-WT_5 (Fig. 5 *a*), BSA-WT_8 (*b*), and nucleoplasmin (*c*). Similar amounts of colloid were injected into each oocyte. Progressing from Fig. 5, *a* to *c*, there is an increase in the number of particles present both within the nucleus and along the envelope. The relationship between the accumulation of particles along the envelope and relative uptake is shown in Table VII. The envelope to cytoplasm ratios were obtained by comparing the number of particles associated with the envelope to the number of particles in an equal, randomly selected area of cytoplasm. It is evident that a direct relationship exists between the number of particles associated with the envelope and nuclear uptake. A similar relationship between uptake and binding was obtained with the 120–280-Å particle fractions, coated with BSA-WT_8, BSA-WT_{11}, or nucleoplasmin (data not shown).

Coinjection of BSA-WT_8– and Nucleoplasmin-coated Particles

To determine if different targeting signals can be transported

*Table V. Size Distribution of BSA-WT_8–, BSA-WT_{11}– and Nucleoplasmin-coated Particles in Injected Cells**

Experiment (1 h)	Total No. of particles measured	Percentage of particles in each size class‡					
		120–145 Å	145–170 Å	170–195 Å	195–220 Å	220–245 Å	>245 Å
BSA-WT_8							
Nucleus	371	3.2	21.6	55.5	18.6	1.1	–
Cytoplasm	556	2.9	16.5	51.3	21.9	5.9	1.4
BSA-WT_{11}							
Nucleus	358	4.2	21.5	53.6	19.6	1.1	–
Cytoplasm	557	3.2	14.7	50.6	22.8	7.0	1.6
Nucleoplasmin							
Nucleus	514	3.5	18.9	55.6	19.0	2.4	–
Cytoplasm	525	3.2	16.4	49.3	20.4	7.2	3.4

* These experiments were performed with 120–280-Å gold particles; the mean size of the fraction was 180 Å.
‡ The size of the gold particles does not include the thickness of the coating agent.

*Table VI. Size Distribution of BSA-WT_8-cT_7– and Large T–Antigen-coated Particles in Injected Cells**

Experiment (1 h)	Total No. of particles measured	Percentage of particles in each size class‡					
		10–30 Å	30–50 Å	50–70 Å	70–90 Å	90–110 Å	>110 Å
Large T–Antigen							
Nucleus	386	22.8	49.0	26.2	2.0	–	–
Cytoplasm	600	16.2	30.3	39.3	8.8	3.7	1.7
BSA-WT_8-cT_7 (1:3 dilution)							
Nucleus	574	26.0	40.1	27.4	5.2	0.7	0.2
Cytoplasm	621	11.6	23.7	37.6	16.7	7.1	3.6

* These experiments were performed with 20–120-Å gold particles; the mean size of the fraction was 60 Å.
‡ The size of the gold particles does not include the thickness of the coating agent.

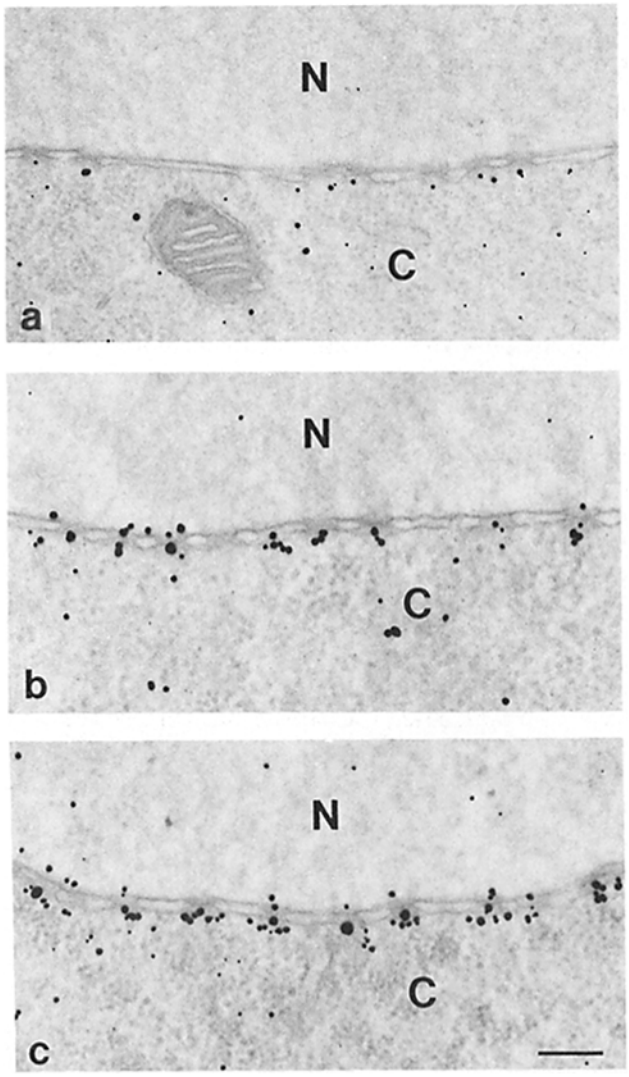

Figure 5. Accumulation of tracers along the nuclear envelope (1-h experiment). A comparison of the intracellular distributions of 50–280-Å gold particles coated with BSA-WT_5 (*a*), BSA-WT_8 (*b*), and nucleoplasmin (*c*). Similar amounts of colloid were injected in each oocyte. Progressing from *a* to *c*, there is an increase in the number of particles present both within the nucleus (*N*) and along the nuclear envelope. *C*, cytoplasm. Bar, 0.2 μm.

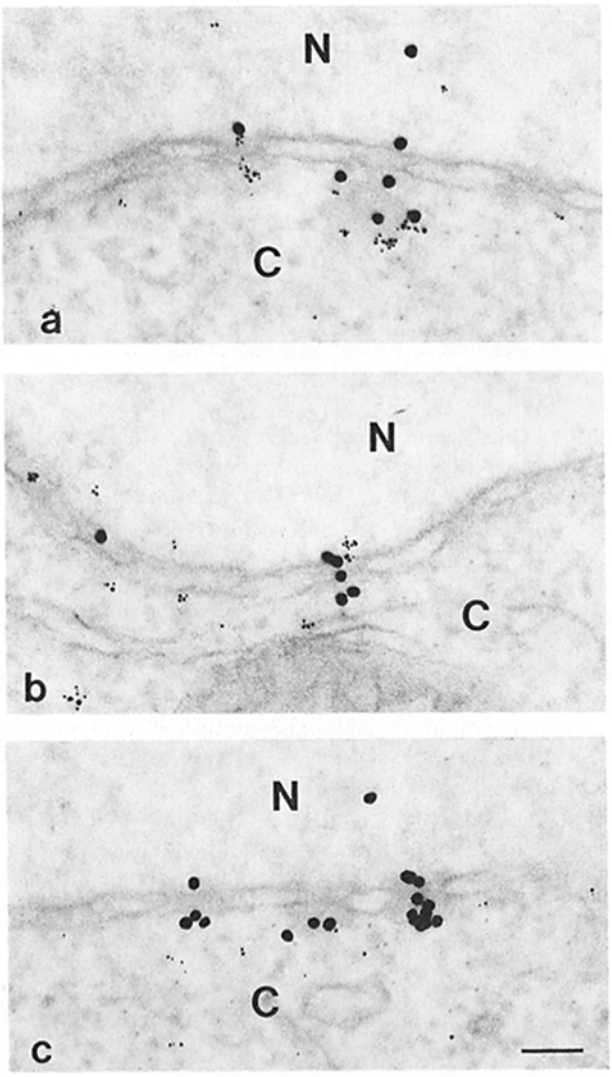

Figure 6. Coinjection of gold particles coated with BSA-conjugates and nucleoplasmin (1-h experiments). (*a* and *b*) Large nucleoplasmin-coated particles (120–280 Å) and small BSA-WT_8–coated particles (20–50 Å) can both be seen within the pore region or just at the nuclear surface of the same pores. (*c*) Large nucleoplasmin-coated particles are seen entering the nucleus (*N*) while small BSA-cT_7–coated particles are retained in the cytoplasm (*C*). Bar, 0.1 μm.

through the same pore, small particles (20–50 Å) coated with BSA-WT_8, and large particles (120–280 Å) coated with nucleoplasmin were injected simultaneously into the cytoplasm. As seen in Fig. 6, *a* and *b*, small and large particles are located either within or adjacent to the nuclear surface of the same nuclear pore. To control for nonspecific binding of the small particles to the large particles, or possible exchange of coat material during the injection procedure, experiments were also performed in which small gold particles were coated with BSA-cT_7 and mixed with the large nucleoplasmin-gold particles before injection. Electron microscopic analysis of this experiment, shown in Fig. 6 *c*, indicates that only large particles are present in the pores and the nucleus while the small tracer particles are retained in the cytoplasm. These experiments demonstrate that individual pores can recognize and translocate different nuclear targeting signals.

Table VII. Envelope-associated Particles

Coating agent	Envelope/cytoplasm ratios*	N/C ratios
BSA-WT_5	1.2	0.06
BSA-WT_8	2.7	0.35
Nucleoplasmin	6.3	0.71

* These ratios were obtained 1 h after injection as described in the text.

Discussion

By stabilizing colloidal gold particles with BSA conjugated with synthetic peptides that contained either active or inactive SV-40 large T-antigen nuclear transport signals, it was possible to prepare a range of electron microscopic tracers that varied in both size and signal content. Electron micro-

scopic analysis of the intracellular distributions of the tracer particles after microinjection into oocytes led to the following conclusions. First, BSA conjugates containing active signals are transported into the nucleus through central channels located within the pores. Second, both the functional size of the channels and relative nuclear uptake increase as the signal number per gold particle increases. Furthermore, the maximum size of the transport channel is estimated to be 260 Å in diameter. Control experiments, using BSA conjugated with inactive signals, demonstrated that differences in the uptake of gold particles coated with different BSA-WT conjugates were due to variations in the number of active signals and not to nonspecific factors such as alterations in particle size and charge.

We found that BSA-cT-gold particles did not accumulate along the outer surface of the envelope and were excluded from the nucleoplasm to the same extent as particles coated with BSA alone. In contrast, Goldfarb et al. (12) and Newmeyer and Forbes (25) reported limited nuclear uptake of proteins conjugated with SV-40 large T signals in which threonine was substituted for lysine[128]. The reason for this disparity is not known, but there are several possible explanations, including differences in (*a*) the ability of threonine and asparagine to block transport, (*b*) the experimental systems that were employed, and (*c*) the number of signals conjugated to each carrier protein.

Nucleoplasmin-coated gold was used as a stabilizing agent to compare the effectiveness of a different nuclear targeting signal. It was found that nucleoplasmin, BSA-WT_8, and BSA-WT_{11} all had similar effects on the functional size of the transport channel, even though nucleoplasmin has fewer signals than either of the conjugates. However, the relative uptake of nucleoplasmin-coated gold was significantly greater than that observed for particles coated with the BSA-WT conjugates. The fact that nucleoplasmin-gold accumulated along the nuclear surface to a greater degree than other tracers suggests that the relative effectiveness of different targeting sequences might be related to their binding affinity for transport receptors.

The possibility that binding might be an important step in the transport process was originally suggested by Feldherr et al. (10), and was based on the observation that nucleoplasmin-gold particles accumulate at the surface of the pores during translocation. Other data in support of this view are the kinetic studies of Goldfarb et al. (12) which demonstrate that the nuclear uptake of BSA conjugated with large T targeting signals is saturable and, therefore, likely to be a receptor-mediated process. Furthermore, Newmeyer and Forbes (25) and Richardson et al. (28) obtained evidence that transport involves two separate events; the first is binding to the pores, which is signal sequence dependent, and the second is translocation into the nucleus, which is ATP dependent.

Overall, the data obtained in this study are consistent with the view that transport occurs through the pores by a gated process. We would suggest that a 90-Å channel is normally present within the pores allowing for the diffusion of smaller macromolecules into and out of the nucleus (26). However, in response to an appropriate transport signal, the dimensions of the channel can increase in size to accommodate the uptake of transportable (nondiffusive) macromolecules.

The results obtained with nucleoplasmin and the BSA conjugates indicate that the extent of channel dilation might be variable and dependent on the number of simultaneous interactions between signals and receptors. Thus, the degree to which the channels are dilated is likely to be modulated by a combination of two factors: (*a*) the number of transport signals available and (*b*) the binding affinity of the signals for the receptors. According to this model, a small number of high affinity signals might be as effective in regulating the size of the transport channel as a larger number of low affinity signals.

In evaluating the effect of signal number on the translocation process, it should be kept in mind that endogenous karyophilic proteins would also contribute to the total pool of transport signals. The degree to which endogenous proteins might influence the uptake of the tracer particles cannot be determined at this time.

Coinjection of different size gold particles, coated with proteins containing different nuclear targeting signals (BSA-WT and nucleoplasmin), demonstrated that individual pores are capable of recognizing and transporting different nuclear targeting signals. In a study to show the bidirectional capability of the nuclear pores, Dworetzky and Feldherr (6) have demonstrated that individual pores can transport both protein and RNA. Whether all transport signals can be recognized by each pore has yet to be determined.

The authors would like to thank Drs. R. Cohen, C. West, G. Stein, and W. Dunn for their critical review of the manuscript.

This work was supported by grant HD20678 from the National Institutes of Health.

Received for publication 2 March 1988, and in revised form 7 June 1988.

References

1. Burglin, T. R., and E. M. De Robertis. 1987. The nuclear migration signal of Xenopus laevis nucleoplasmin. *EMBO (Eur. Mol. Biol. Organ.) J.* 6:2617–2625.
2. De Roe, C., P. J. Courtoy, and P. Baudhuin. 1987. A model of protein-colloidal gold interactions. *J. Histochem. Cytochem.* 35:1191–1198.
3. Dingwall, C., S. M. Dilworth, S. J. Black, S. E. Kearsey, L. S. Cox, and R. A. Laskey. 1987. Nucleoplasmin cDNA sequence reveals polyglutamic acid tracts and a cluster of sequences homologous to putative nuclear localization signals. *EMBO (Eur. Mol. Biol. Organ.) J.* 6:69–74.
4. Dingwall, C., S. V. Sharnick, and R. A. Laskey. 1982. A polypeptide domain that specifies migration of nucleoplasmin into the nucleus. *Cell.* 30:449–458.
5. Dumont, J. N. 1972. Oogenesis in Xenopus laevis (Daudin). I. Stages of oocyte development in laboratory maintained animals. *J. Morphol.* 136: 153–179.
6. Dworetzky, S. I., and C. M. Feldherr. 1988. Translocation of RNA-coated gold particles through the nuclear pores of oocytes. *J. Cell Biol.* 106: 575–584.
7. Feldherr, C. M. 1965. The effect of the electron-opaque pore material on exchanges through the nuclear annuli. *J. Cell Biol.* 25:43–53.
8. Feldherr, C. M. 1975. The uptake of endogenous proteins by oocyte nuclei. *Exp. Cell Res.* 93:411–419.
9. Feldherr, C. M., R. J. Cohen, and J. A. Ogburn. 1983. Evidence for mediated protein uptake by amphibian oocyte nuclei. *J. Cell Biol.* 96:1486–1490.
10. Feldherr, C. M., E. Kallenbach, and N. Schultz. 1984. Movement of a karyophilic protein through the nuclear pores of oocytes. *J. Cell Biol.* 99:2216–2222.
11. Frens, G. 1973. Controlled nucleation for the regulation of the particle size in monodisperse gold suspensions. *Nature Phys. Sci.* 241:20–22.
12. Goldfarb, D. S., J. Gariepy, G. Schoolnik, and R. D. Kornberg. 1986. Synthetic peptides as nuclear localization signals. *Nature (Lond.).* 322: 641–644.
13. Hall, M. N., L. Hereford, and I. Herskowitz. 1984. Targeting of E. coli β-galactosidase to the nucleus in yeast. *Cell.* 36:1057–1065.
14. Kalderon, D., W. D. Richardson, A. F. Markham, and A. E. Smith. 1984. Sequence requirements for nuclear localization of simian virus 40 large-T antigen. *Nature (Lond.).* 311:33–38.
15. Kressman, A., and M. L. Birnstiel. 1980. Surrogate genetics in the frog oocyte. *In* Transfer of Cell Constituents into Eukaryotic Cells. J. E. Celis, A. Graessmann, and A. Loyter, editors. Plenum Publishing Corp.,

New York. 383–407.
16. Lanford, R. E., and J. S. Butel. 1984. Construction and characterization of an SV40 mutant defective in nuclear transport of T antigen. *Cell.* 37:801–813.
17. Lanford, R. E., P. Kanda, and R. C. Kennedy. 1986. Induction of nuclear transport with a synthetic peptide homologous to the SV40 T antigen transport signal. *Cell.* 46:575–582.
18. Lanford, R. E., R. G. White, R. G. Dunham, and P. Kanda. 1988. Effects of basic and nonbasic amino acid substitutions on transport induced by SV40 T antigen synthetic peptide nuclear transport signals. *Mol. Cell. Biol.* 8:2722–2729.
19. Luckow, V. A., and M. D. Summers. 1988. Trends in the development of bacolovirus expression vectors. *Bio/Technology.* 6:47–55.
20. Lyons, R. H., B. Q. Ferguson, and M. Rosenberg. 1987. Pentapeptide nuclear localization signal in adenovirus E1a. *Mol. Cell. Biol.* 7:2451–2456.
21. Merrifield, R. B. 1963. Solid phase peptide synthesis. I. The synthesis of a tetrapeptide. *J. Am. Chem. Soc.* 85:2149–2154.
22. Miller, D. S., Y. T. Lau, and S. B. Horowitz. 1984. Artifacts caused by cell microinjection. *Proc. Natl. Acad. Sci. USA.* 81:1426–1430.
23. Moreland, R. B., G. L. Langevin, R. H. Singer, R. L. Garcea, and L. M. Hereford. 1987. Amino acid sequences that determine the nuclear localization of yeast histone 2B. *Mol. Cell. Biol.* 7:4048–4057.
24. Moreland, R. B., H. G. Nam, L. M. Hereford, and H. M. Fried. 1985. Identification of a nuclear localization signal of a yeast ribosomal protein. *Proc. Natl. Acad. Sci. USA.* 82:6561–6565.
25. Newmeyer, D. D., and D. J. Forbes. 1988. Nuclear import can be separated into two distinct steps in vitro: nuclear pore binding and translocation. *Cell.* 52:641–653.
26. Paine, P. L. 1975. Nucleocytoplasmic movement of fluorescent tracers microinjected into living salivary gland cells. *J. Cell Biol.* 66:652–657.
27. Paine, P. L., L. C. Moore, and S. B. Horowitz. 1975. Nuclear envelope permeability. *Nature (Lond.).* 254:109–114.
28. Richardson, W. D., A. D. Mills, S. M. Dilworth, R. A. Laskey, and C. Dingwall. 1988. Nuclear protein migration involves two steps: rapid binding at the nuclear envelope followed by slower translocation through nuclear pores. *Cell.* 52:655–664.
29. Richardson, W. D., B. L. Roberts, and A. E. Smith. 1986. Nuclear location signals in polyoma virus large-T. *Cell.* 44:77–85.
30. Roberts, B. L., W. D. Richardson, and A. E. Smith. 1987. The effect of protein context on nuclear location signal function. *Cell.* 50:465–475.
31. Schulz, B., and R. Peters. 1986. Intracellular transport of a karyophilic protein. *In* Nucleocytoplasmic Transport. R. Peters and M. Trendelenburg, editors. Springer-Verlag, Berlin. 171–184.
32. Siamins, V., and D. P. Lane. 1985. An immunoaffinity purification procedure for SV 40 large T-antigen. *Virology.* 144:88–100.
33. Silver, P. A., L. P. Keegan, and M. Ptashne. 1984. Amino terminus of the yeast GAL4 gene product is sufficient for nuclear localization. *Proc. Natl. Acad. Sci. USA.* 81:5951–5955.
34. Sugawa, H., N. Imamoto, M. Wataya-Kaneda, and T. Uchida. 1985. Foreign protein can be carried into the nucleus of mammalian cell by conjugation with nucleoplasmin. *Exp. Cell Res.* 159:419–429.